"Click" dendrimer-Pd nanoparticle assemblies as enzyme mimics: Catalytic o-phenylenediamine oxidation and application to colorimetric H2O2 detection

Journal:	*Inorganic Chemistry Frontiers*
Manuscript ID	Draft
Article Type:	Research Article
Date Submitted by the Author:	n/a
Complete List of Authors:	Liu, Yue; Univ. Bordeaux Lopes, Renata; Federal University of Viçosa, Chemistry Lüdtke, Tanja; CIC biomaGUNE Di Silvio, Desire; CIC biomaGUNE, Biointerfaces Moya, Sergio; CIC biomaGUNE, Biointerfaces Hamon, Jean-Rene; UMR 6226 CNRS-Universite de Rennes 1, Sciences Chimiques de Rennes Astruc, Didier; Univ. Bordeaux,

SCHOLARONE™
Manuscripts

ARTICLE

"Click" dendrimer-Pd nanoparticle assemblies as enzyme mimics: Catalytic *o*-phenylenediamine oxidation and application to colorimetric H₂O₂ detection

Yue Liu,[a] Renata Pereira Lopes,[a,b,*] Tanja Lüdtke,[c] Desire Di Silvio,[c] Sergio Moya,[c] Jean-René Hamon,[d] Didier Astruc[a,*]

Dendrimers have already successfully been used in nanoparticle (NP) catalysis for many years, particularly for Pd NP protection for carbon-carbon coupling reactions. In this paper, assemblies between Pd nanoparticles and two generations of "click" dendrimers, with respectively 27 (dendrimer-**1**) and 81 (dendrimer-**2**) triethylene glycol (TEG) termini are examined for catalytic peroxidase-like oxidative activity. This catalysis is investigated with o-phenylenediamine (OPD) and H₂O₂ as the substrates in water, displaying different colours. The dendrimer effect is negative upon increasing generation, i.e., dendrimer **1**-Pd nanoparticles show the best results, providing values with a V_{max} of 1.51×10^{-9} M s^{-1} and K_m of 3.06 mM as obtained with the Michaelis-Menten model. The detection limit is 0.82 µM of H₂O₂ detection with dendrimer-**1**-PdNPs, and both dendrimer-Pd nanocatalysts exhibit excellent robustness of catalytic activity, a water-dispersive state being stable for at least 2 months, thus showing a promising mimic as peroxidase catalysts.

Introduction

Hydrogen peroxide (H₂O₂) is a strong oxidant, appearing as a beenby-product of many oxidase enzymes. Thereby, it is an important mediator in food, pharmaceutical, clinical, industrial and environmental analysis.[1-5] Peroxidase enzymes uses H₂O₂ to catalyse substrate oxidation. Peroxidase activity can be as well used for the detection of hydrogen peroxide, which is essential to biochemical analysis for application in biological and environmental processes. [6,7] Natural enzymes, such as for example horseradish peroxidase (HRP),[8] have the disadvantages of expensive cost and complex preparation. As a result, much work has been devoted to produce stable, highly sensitive and low-cost enzyme mimics as H₂O₂ biosensors. Since Gao et al. first reported that Fe₃O₄ nanoparticles (NPs) could be used to detect H₂O₂ and showed peroxidase-like activity similar to HRP,[9] various nanomaterials have been proposed as enzyme mimics in the detection of hydrogen peroxide, such as magnetic NPs,[5,10,11] silver alloys nanostructure,[4] Au@Pt nanostructures,[12] and ruthenium nanomaterials.[13]

There are examples of dendrimers[14-16] that have proposed as enzyme mimics.[17,18] Dendrimer-RNA NPs have been shown to generate protective immunity against several lethal viruses.[19] Polyamidoamine (PAMAM) dendrimers with encapsulated metal NPs have also been shown to function as catalysts for some reactions,[20,21] and this principle has been extended to some other dendrimer families.[22,25] In particular "click" dendrimers synthesized by CuAAC "click" reactions between azido-terminated dendrimers and alkynes show excellent performances as catalytic NP supports due to their encapsulating properties and compromise between the stabilising triazole coordination to transition metals and freedom of nanoparticle surface sites.[26-29]

We report here "click" dendrimer-palladium (Pd) NPs as peroxidase enzyme mimics of H₂O₂ sensing using o-phenylenediamine (OPD) oxidation by H₂O₂ to 2,3-diaminophenazine (DAP). Pd NPs that do not require sophisticated ligands are among the best NPs in catalysis, and their catalytic properties, comparable to those of molecular catalysts, are already well known.[29-32,33] The two "click" dendrimers used here are known[27,34] and contain respectively 27 (dendrimer-**1**) and 81 (dendrimer-**2**) triethylene glycol (TEG) termini and 9 and 27 1,2,3-triazole ligands (Figure 1). So far, dendrimer-NP assemblies have not yet been employed as peroxidase enzyme mimics. Equation **1** shows the oxidation of *o*-phenylenediamine (OPD) by H₂O₂ forming 2,3-diaminophenazine (DAP) in the presence of the Pd-dendrimer

[a.] *ISM, UMR CNRS Nº 5255, Univ. Bordeaux, 33405 Talence Cedex, France. E-mail: yue.liu@u-bordeaux.fr, didier.astruc@u-bordeaux.fr*

[b.] *Department of Chemistry, Universidade Federal de Viçosa, Viçosa/MG, Brazil, 36570-900. E-mail: renataplmoreira@gmail.com*

[c.] *Soft Matter Nanotechnology Lab, CIC biomaGUNE, Paseo Miramón 182, 20014 Donostia-San Sebastián, Gipuzkoa, Spain*

[d.] *Institut des Sciences Chimiques, UMR CNRS 6226, Université de Rennes 1, 35042 Rennes Cedex, France*

nanocatalysts. The impact of OPD concentration, H_2O_2 concentration and pH as well as the role of dendrimer generation are assessed to determine their influence on the peroxidase-like activity.
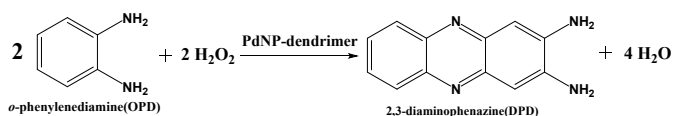
Eq.1

Experimental

Chemicals and reagents

Sodium hydroxide, sodium borohydride, disodium tetrachloropalladate palladium acetate, hydrogen peroxide, o-phenylenediamine and sodium citrate dihydrate were obtained from Sigma-Aldrich. Ultrapure water (Thermo Fisher Scientific INC., USA) was utilized for the preparation of all aqueous solutions.

Synthesis of the dendrimer-1-PdNPs and dendrimer-2-PdNPs assemblies

Dendrimer-**1** and dendrimer-**2** (Fig. 1) have been synthesized following a previous report.[34] The ^1H NMR spectra of dendrimer-**1** and dendrimer-**2** are shown in Fig. S1 and Fig. S2. The nanocatalyst dendrimer-**1**-PdNPs and dendrimer-**2**-PdNPs were prepared by a facile one-step method. Typically, dendrimer-**1** (0.4 mg, 1.5 equiv. TEG branch per metal) dissolved in 1 mL water and Na_2Cl_4Pd (2.94 mg, 1 equiv) dissolved in 1 mL water were mixed in 2 mL water by magnetic stirring for 30 min at room temperature (rt ~25 °C), then 1 mL of freshly prepared $NaBH_4$ aqueous solution (10 equiv. per metal) was quickly added. The mixture was allowed to stir for 30 min at rt, and the resulting nanocatalyst was directly used *in situ* without further treatment. For the synthesis of dendrimer-**2**-PdNPs, the steps are similar to those used for dendrimer-**1**-PdNPs, the molar ratio of Pd: TEG branch: $NaBH_4$ is 1: 1.5: 10.

Fig. 1 Molecular structures of dendrimer **1** and dendrimer **2**.

General procedure for oxidation of *o*-phenylenediamine

In a quartz cuvette with 1 cm optical path, were added 0.4 mL of H_2O_2 30%, 0.2 mL of OPD solution (0.1 mol L^{-1}, (freshly prepared) and 2 mL of citrate buffer (pH 3.0). For the pH study, the pH of the citrate solution was adjusted to 5 and 7 by addition of a small amount of HCl. Then, 0.1 mL dendrimer-**1**-PdNPs or dendrimer-**2**-PdNPs were added to the system.

For the synthesis of Pd/Fe_3O_4@dendrimer-**1**, dendrimer-**1** (0.4 mg, 1.5 equiv. TEG branch per metal) dissolved in 1 mL water and Fe_3O_4 (0.23 mg, 1 equiv per metal) were mixed in 1 mL water by magnetic stirring for 20 min at rt, then Na_4Cl_2Pd (2.94 mg, 1 equiv) dissolved in 1 mL water was added. The reaction mixture was stirred for 10 min, then 1 mL of freshly prepared aqueous solution of $NaBH_4$ (10 equiv. per metal) was quickly added. The mixture was allowed to stir for 30 min at rt.

The reactions were monitored by UV-vis. spectroscopy (Varian Cary 100 scan) in full scan mode (350-600 nm) in the interval of 30 min at 22 °C. A new band at 450 nm started to increase in the presence of the catalyst indicating the formation of the oxidation product (DAP). The absorbance data were converted to DAP concentration using the extinction coefficient (log ε_{450} = 4.33).[35] The effect of OPD concentration (1.725 - 17.25 mM), H_2O_2 concentration (6.3 - 75.6 μM) and pH (3.0 - 7.0) were assessed to determine their influence on the peroxidase-like activity.

The limit of detection (LD) was calculated using Eq. **2**.

$$LD = \frac{3 \times \text{standard deviation of blanc}}{\text{sensitivity of the analytical curve}}$$

Eq. **2**

The Michaelis Menten model, usually employed to model enzymatic reactions with substrate concentration in excess, was adjusted to the experimental data in order to obtain the kinetic parameters V_{max} and K_m (Eq. **3**).

$$V_0 = \frac{V_{max} \cdot [S]}{K_m + [S]}$$

Eq. **3**

Therein, V_0 is the initial reaction rate, V_{max} the maximum reaction rate, K_m is the Michaelis constant which represents the affinity of enzyme toward substrate, the value of K_m being equal to the substrate concentration at which the reaction rate is half of the maximum reaction rate. And [S] is the substrate concentration.

Results

Characterization of the nanomaterials

Dendrimer-**1**-PdNPs and dendrimer-**2**-PdNPs were fabricated in a one-step process in which $NaBH_4$ acted as the reductant of Na_2PdCl_4. The triazole groups in the dendrimers terminated by 27 resp. 81 triethylene glycol (TEG) termini (Fig. 1) stabilized the Pd NPs. The obtained Pd NPs were characterized by TEM and XPS. The average size of dendrimer-**1**-PdNPs determined by TEM is 2.5 ± 1 nm, and the shape of the Pd NP core is quasi-spherical (Fig. 3a). Dendrimer-**2**-PdNPs also showed a quasi-spherical shape with a size of 3.6 ± 2 nm (Fig. 2b).

The dendrimers were further characterized by XPS measurements to investigate the surface composition (Fig. 3 for
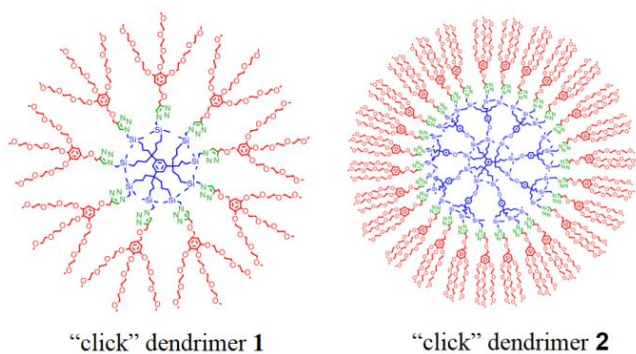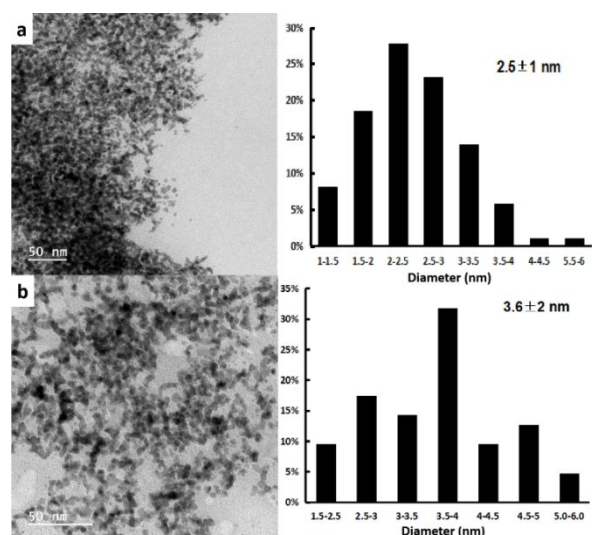
Fig. 2 Transmission Electronic Microscopy (TEM) of a) dendrimer-**1**-PdNPs; Pd NPs size: 2.9 ± 1 nm; b) dendrimer-**2**-PdNPs; Pd NPs size: 3.6 ± 1.5 nm.

dendrimer-**1**-PdNPs and Fig. S3-S6 and Table S1-S2 for dendrimer-**2**-PdNP). The bands at 284.8, 286.4, 288.2 and 289.4 eV in the C1s spectra for dendrimer-**1**-PdNPs correspond to C-C, C-O/C-N, C=O and O-C=O, respectively. The band N 1s in 400.4 eV is assigned to N-C binding, whereas the band O 1s in 532.4 eV is attributed to C=O binding. In the Pd 3d spectra of dendrimer-**1**-PdNPs, the band at 334.8 eV is assigned to Pd(0) NPs, whereas the bands at 335.5 and 337.4 eV are assigned to Pd^{II} (with two distinct types). These results further support the successful formation of Pd NPs with dendrimer generations.
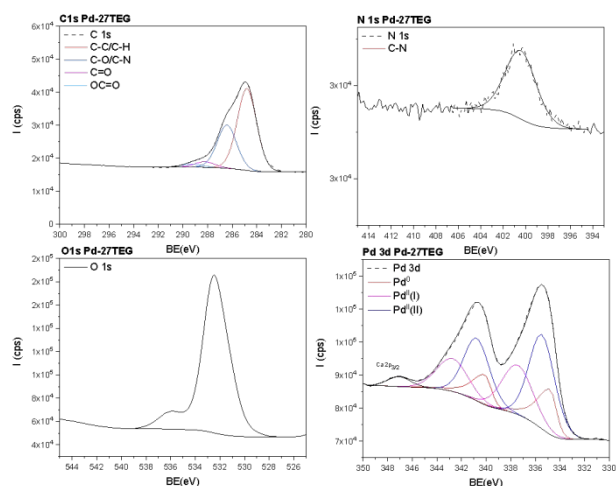

Fig. 3 XPS signal from (a) C 1s of dendrimer-**1**-PdNPs (b) N 1s of dendrimer-**1**-PdNPs (c) O 1s of dendrimer-**1**-PdNPs and (d) Pd 3d of dendrimer-**1**-PdNPs.

Nanocatalysed oxidation of *o*-phenylenediamine

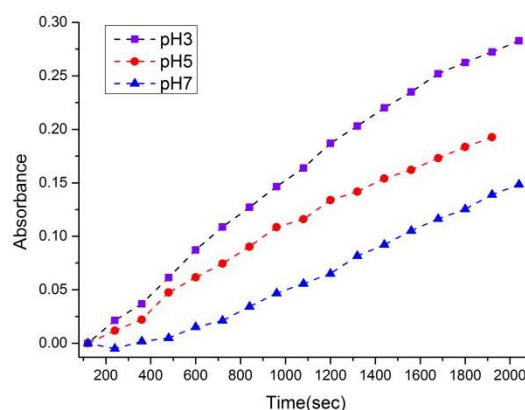Several factors affect the catalytic activity of OPD oxidation including the solution pH, OPD concentration and H_2O_2

Fig. 4 OPD oxidation by dendrimer-**1**-PdNPs at various pH values. General conditions: 0.1 M OPD; 10 mM H_2O_2 30%; 2 mM dendrimer-**1**-PdNPs.

concentration. The pH effects on the reaction are shown in Fig. 4 and Fig. S11 (Supporting Information).

The activity increased with decreasing pH from 7.0 to 3.0, with the maximum absorbance being found at pH 3.0. The reaction rate decreases
in the order pH 3.0 > pH 5.0 > pH 7.0 (Fig. 4). This indicates that, for pH 3.0, the maximum absorption wavelength in the UV-vis. spectrum is 450 nm (Fig. S7). Upon pH increase from 3.0 to 7.0, a hypsochromic shift is observed, with a maximum absorption at 412 nm for pH 7.0. This effect is associated to the chemical behaviour of the DAP molecule whose pK_{a1} is 1.0-2.0 and pK_{a2} is 5.1.[36] Therefore, for the other experiments, pH was fixed at 3.0. Both dendrimer generations (dendrimers **1** and **2**) were used to stabilize the Pd NPs and applied in the OPD oxidation reaction. Besides that, the fresh and two-month-old PdNP@dendrimer were compared, and the addition of magnetic Fe_3O_4 NPs on PdNP@dendrimer was also evaluated. The experiments were performed at pH 3.0 in order to evaluate the effect of different catalysts in the OPD oxidation reaction, and the results are shown in Fig. 5.

In 80 minutes of reaction, the efficiency followed the order: dendrimer-**1**-PdNPs (aged 2 months) < Pd/Fe$_3$O$_4$@dendrimer-**1** < dendrimer-**2**-PdNPs < dendrimer-**1**-PdNPs. These results show that dendrimer-**1**-PdNPs is the best catalyst. Besides, there is a negative influence of Fe_3O_4 on the catalyst dendrimer-**1**-PdNPs, i.e., the peroxidase-like activity of Fe_3O_4/dendrimer-**1**-PdNPs is not as good as that of dendrimer-**1**-PdNPs, although Fe_3O_4 has often been used previously as support for this type of reaction.[5,9,10]

Importantly, dendrimer-**1**-PdNPs was used in water-dispersive state at least 2 months and then still possessed peroxidase-like catalytic activity.[37]

The third parameter that was evaluated in the OPD oxidation reaction, using the dendrimer-**1**-PdNPs, was the OPD concentration. According to the UV-vis. curve (Fig. S8 and Fig. S9), the colour of the solution changes with the increase of OPD concentration, and the reaction kinetics was found to follow the Michaelis-Menten model (Fig. 6). The V_{max} and K_m values
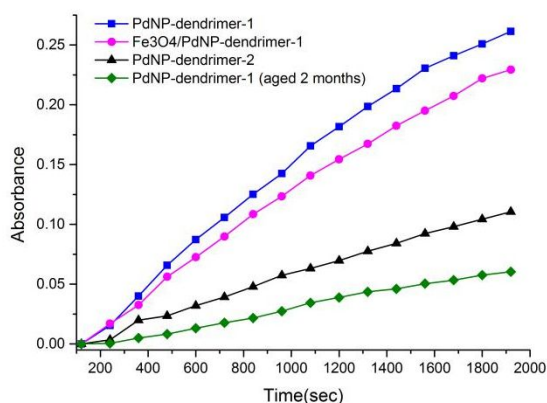
Fig. 5 OPD oxidation by dendrimer-**1**-PdNPs, dendrimer-**2**-PdNPs and dendrimer-**1**-PdNPs (aged 2 months). General conditions: 0.1 M OPD; 10 mM H_2O_2 30%; 2 mM of the catalyst and pH 3.0

obtained were, respectively, 1.51×10^{-9} M s^{-1} and $K_m = 3.06$ mM. V_{max} is an indicator of the catalytic activity, whereas K_m indicates the affinity of the catalyst for the substrate.[8,38] The values of V_{max} and K_m are favourably comparable to those of other materials as shown in Table S3.The system was used for the quantification of H_2O_2 and, for this purpose, an analytical curve was constructed (Fig. 7). A satisfactory correlation was observed (correlation coefficient > 0.9), and the absorbance of oxidized OPD increased with the increase of the H_2O_2 concentration (Fig. 7a). Meanwhile, these changes with the increase of H_2O_2 concentration were observed by the naked eye (Fig. 7b), the solution containing the dendrimer-**1**-PdNPs becoming yellow-orange from colourless. There is a linear relationship between the absorbance of oxidized OPD concentration ranging from 6.3 to 75.6 μM (Fig. 7c), and this reaction kinetics also followed the Michaelis-Menten model. The V_{max} and K_m values obtained were, respectively, 1.06×10^{-8} M s^{-1} and 9.04 mM. The detection limit for dendrimer-**1**-PdNPs was found to be 0.5 μM (Table 1). These parameters are compared to those reported in other studies of the literature (Table 1).

Discussion

The "click" dendrimers being known as excellent templates for late transition-metal NPs, and particularly Pd NPs, they were certainly good candidates as enzyme mimics when associated to Pd NPs. The "click" dendrimers **1** and **2** therefore stabilise very small PdNPs due to the intra-dendritic triazole coordination. Such a small NP size is a condition for good efficiency, since the efficiency is related to the total NP surface. Another parameter to consider is the substrate access to the PdNP surface. With the dendrimers, the intra-dendritic location of the PdNPs may introduce a steric constraint for substrate access to the PdNP surface. The dendritic effect involving a lower reaction rate of the larger dendrimer-**2**-PdNPs compared to dendrimer-**1**-PdNPs may be taken into account by this parameter. Finally, the H_2O_2 concentration is also directly related to the peroxidase-like catalytic reaction rate. Therefore,
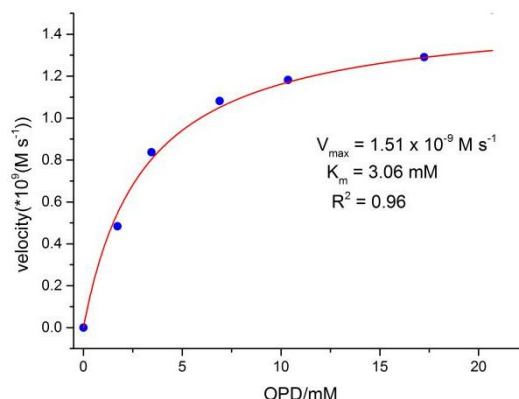

Fig. 6 [OPD]-Velocity curve obtained using the Michaelis–Menten model. General conditions: 10 mM H_2O_2 30%; 2 mM dendrimer-**1**-PdNPs and pH 3.0
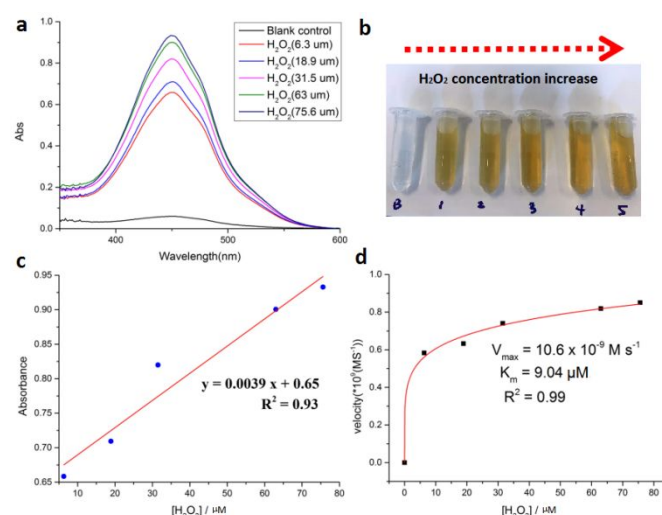

Fig. 7 Variation of the H_2O_2 concentration with dendrimer-**1**-PdNPs. General conditions: 0.1M OPD; 2 mM dendrimer-**1**-PdNPs. (a. UV-vis. spectra for various H_2O_2 concentrations; b. colour changes of oxidized OPD in the presence of dendrimer-**1**-PdNPs with H_2O_2 at various concentrations; c. linear calibration plots of absorbance of oxidized OPD at 450 nm; d. [H_2O_2] velocity curve using the Michaelis-Menten model).

reaction rates recorded here were lower than in some other reports, which is are directly caused by H_2O_2 concentration that was lower in the present study. The values obtained here are comparable to the best literature data, demonstrating that the present nanocatalyst not only has a comparable lower detection limit, but also possesses the advantages of excellent water dispersion and stability, which emphasizes the potential of dendrimer-**1**-PdNPs to function as an excellent catalyst in peroxidase-like reactions. Table 1 concerns only OPD for comparison with the results obtained in this work. Catalyst.

Table 1. Comparison of the analytical parameters for the quantification of H_2O_2 reported in other nanomaterial-based enzyme mimics.

Catalyst	Linear range (µM)	Detection limit (µM)	pH	Reaction Temperature	Ref.
Ag-CoO NPs	5 - 20	3.47	5.0	r.t.*	[4]
MnFe$_2$O$_4$	100 - 15000	30	7.0	r.t.*	[38]
Fe$_3$O$_4$@Cu@ Cu$_2$O	400 - 1500	200	8.0	25 °C	[39]
CuS nanorods	1.0 - 1000	0.11	4.0	45 °C	[40]
Cu co-doped carbon dots	5 - 200	1.1	6.0	35 °C	[41]
dendrimer-**1**-PdNPs	6.3 - 75.6	0.5	3.0	22 °C	This work

*Room temperature

mimicking peroxidase have sometimes also previously been used for 3,3',5,5'-tetramethylbenzidine. [8,42-44]

Since the diameter size of dendrimer **1** is about 10 nm,[27,28] the smallest PdNPs are much smaller than the dendrimers and stabilised by the intradendritic triazole ligands along the dendritic triazole tethers, whereas larger PdNPs are most probably stabilised inter-dendritically. Concerning dendrimer-**2** PdNPs, their dispersity is clearly, from the TEM images, much larger than that of the dendrimer-**1**-PdNPs, with a size culminating around 3.6 nm. The kinetic results with dendrimer-**1**-PdNPs show that they are more efficient than dendrimer-**2**-PdNPs due to their small size and easier access of substrates in less bulky tethers.

Conclusion

Stable "click" dendrimer-Pd NP assemblies, utilizing the synergy between intradendritic triazole coordination to the Pd NP surface and bulk of the dendritic core, tethers and cavities, mimic peroxidase enzyme for OPD oxidation in aqueous solutions. A typical Michaelis–Menten kinetics is observed for the reaction in the presence of the dendrimer-Pd NP assemblies with a low detection limit of H_2O_2. Comparison with literature results indicates that the performances reached in H_2O_2 detection using this excellent method are among the very best ever obtained. With these advantages, the optimized dendrimer-**1**-PdNP nano-assembly is a promising biomimetic nanocatalyst with possible other applications in biosensing and environmental monitoring.

Conflicts of interest

There are no conflicts of interest to declare.

Acknowledgements

Notes and references

1   M. Zayats, R. Baron, I. Popov and I. Willner, Biocatalytic growth of Au nanoparticles: from mechanistic aspects to biosensors design, *Nano Lett.,* 2005, **5**, 21–25.

2   T. Preston, W. Muller and G. Singh, Scavenging of extracellular H_2O_2 by catalase inhibits the proliferation of HER-2/Neu-transformed rat-1 fibroblasts through the induction of a stress response, *J. Biol. Chem.*, 2001, **276**, 9558–9564.

3   G. DeYulia, J. Carcamo, O. Borquez-Ojeda, C. Shelton and D. Golde, Hydrogen peroxide generated extracellularly by receptor–ligand interaction facilitates cell signaling, *Proc. Natl. Acad. Sci. U.S.A.*, 2005, **10**, 5044–5049.

4   J. Lian, D. Yin, S. Zhao, X. Zhu, Q. Liu, X. Zhang and X. Zhang, Core-shell structured Ag-CoO nanoparticles with superior peroxidase-like activity for colorimetric sensing hydrogen peroxide and o-phenylenediamine, *Colloids Surfaces A Physicochem. Eng. Asp.*, 2020, **603**, 125283-125292.

5   N. Xiao, S. Liu, S. Mo, Y. Yang, L. Han, Y. Ju, N. Li and H. Luo, B,N-carbon dots-based ratiometric fluorescent and colorimetric dual-readout sensor for H_2O_2 and H_2O_2-involved metabolites detection using ZnFe$_2$O$_4$ magnetic microspheres as peroxidase mimics, *Sensors Actuat., B Chem.*, 2018, **273**, 1735–1743.

6   Q. Li, G. Tang, X. Xiong, Y. Cao, L. Chen, F. Xu and H. Tan, Carbon coated magnetite nanoparticles with improved water-dispersion and peroxidase-like activity for colorimetric sensing of glucose, *Sensor. Actuat. B Chem.*, 2015, **215**, 86–92.

7   X. Chen, B. Su, Z. Cai, X. Chen and M. Oyama, PtPd nanodendrites supported on graphene nanosheets : A peroxidase-like catalyst for colorimetric detection of H_2O_2, *Sens. Actuators B Chem.*, 2014, **201**, 286–292.

8   N. Li, Y. Yan, B. Xia, J. Wang and X. Wang, Novel tungsten carbide nanorods: An intrinsic peroxidase mimetic with high activity and stability in aqueous and organic solvents, *Biosens. Bioelectron.*, 2014, **54**, 521–527.

9   L. Gao, J. Zhuang, L. Nie, J. Zhang, Y. Zhang, N. Gu, T. Wang, J. Feng, D. Yang, S. Per-rett and X. Yan, Intrinsic peroxidase-like activity of ferromagnetic nanoparticles, *Nat. Nanotechnol.*, 2007, **2**, 577–583.

10 Y. Liu and F. Yu, Substrate-specific modifications on magnetic iron oxide nanoparticles as an artificial peroxidase for improving sensitivity in glucose detection, *Nanotechnology*, 2011, **22**, 145704-145712.

11 J. Yin, H. Cao and Y. Lu, Self-assembly into magnetic Co$_3$O$_4$ complex nanostructures as peroxidase, *J. Mater. Chem.*, 2012, **22**, 527–534.

12 W. He, Y. Liu, J. Yuan, J. Yin, X. Wu, X. Hu, K. Zhang, J. Liu, C. Chen, Y. Ji and Y. Guo, Au@Pt nanostructures as oxidase and peroxidase mimetics for use in immunoassays, *Biomaterials*, 2011, **32**, 1139–1147.

13 G. Cao, X. Jiang, H. Zhang, T. Croley and J. Yin, Mimicking horseradish peroxidase and oxidase using ruthenium nanomaterials, *RSC Adv.*, 2017, **7**, 52210–52217.

14 D. A. Tomalia, A. M. Naylor and W. A. Goddard III, Starburst Dendrimers-Molecular Control of Size, Shape, Surface Chemistry, Topology, and Flexibility from Atoms to

Macroscopic Matter, *Angew. Chem., Int. Ed. Engl.*, 1990, **29**, 138-175.

15 G. R. Newkome, C. N. Moorefield and F. Vögtle, *Dendrimers and Dendrons. Concepts, Syntheses, Applications*, Wiley-VCH, Weinheim, 2001.

16 D. Astruc, E. Boisselier and C. Ornelas, Dendrimers Designed for Functions: From Physical, Photophysical, and Supramolecular Properties to Applications in Sensing, Catalysis, Molecular Electronics, Photonics, and Nanomedicine, *Chem. Rev.*, 2010, **110**, 1857-1959.

17 S. Sevenson and D. A. Tomalia, Dendrimers in biomedical applications-reflections on the field, *Adv. Drug Deliv. Rev.*, 2012, **64**, 102-115.

18 C. Deraedt and D. Astruc, Supramolecular nanoreactors for catalysis, *Coord. Chem. Rev.*, 2016, **324**, 106-122.

19 J. S. Chahal, O. F. Khan, C. L. Cooper, J. S. McPartlan, J. K. Tsosie, L. D. Tilley, S. M. Sidik, S. Lourido, R. Langer, S. Bavari, H. Ploegh and D. G. Anderson, Dendrimer-RNA nanoparticles generate protective immunity against lethal Ebola, H1N1 influenza, and Toxoplasma gondii challenges with a single dose, *Proc. Natl. Acad. Sci. USA*, 2016, **113**, E4133–E4142.

20 R. W. Scott, O. M. Wilson and R. M. Crooks, Synthesis, characterization, and applications of dendrimer-encapsulated nanoparticles, *J. Phys. Chem. B*, 2005, **109**, 692-704.

21 V. S. Myers, M. G. Weir, E. V. Carino, D. F. Yancey S. Pande and R. M. Crooks, Dendrimer-encapsulated nanoparticles: New synthetic and characterization methods and catalytic applications, *Chem. Sci.*, 2011, **2**, 1632-1646.

22 A. Balanta, C. Godard and C. Claver, Pd nanoparticles for C–C coupling reactions, *Chem. Soc. Rev.*, 2011, **40**, 4973-4985.

23 K. Yamamoto, T. Imaoka, M. Tanabe and T. Kambe, New Horizon of Nanoparticle and Cluster Catalysis with Dendrimers, *Chem. Rev.*, 2020, **120**, 1397-1437.

24 I. Favier, D. Pla and M. Gomez, Palladium Nanoparticles in Polyols: Synthesis, Catalytic Couplings, and Hydrogenations. *Chem. Rev.*, 2020, **120**, 1146-1183.

25 Z. B. Shifrina, V. G. Matveeva and L. M. Bronstein, Role of Polymer Structures in Catalysis by Transition Metal and Metal Oxide Nanoparticle Composites, *Chem. Rev.*, 2020, **120**, 1350-1396.

26 D. Wang, C. Deraedt, J. Ruiz and D. Astruc, Magnetic and Dendritic Catalysts, *Acc. Chem. Res.*, 2015, **48**, 1871-1880.

27 C. Deraedt, N. Pinaud and D. Astruc, A Recyclable Catalytic Dendrimer Nanoreactor for Part-Per-Million Cu(I) Catalysis of "click" Reactions in Water, *J. Am. Chem. Soc.*, 2014, **136**, 12092-12098.

28 X. Liu, D. Gregurec, J. Irigoyen, A. Martinez, S. Moya, R. Ciganda, P. Hermange, J. Ruiz and D. Astruc, Precise Localization of Metal Nanoparticles in Dendrimer Nanosnakes or Inner Periphery and Consequences in Catalysis, *Nat. Commun.*, 2016, **7**, 13152.

29 D. Astruc, F. Lu and J. Ruiz, Nanoparticles as Recyclable Catalysts: The Fast-growing Frontier between Homogeneous and Heterogeneous Catalysts, *Angew. Chem. Int. Ed.*, 2005, **44**, 7852-7872.

30 C. Deraedt, L. Salmon, L. Etienne, J. Ruiz and D. Astruc, "Click" dendrimers as efficient nanoreactors in aqueous solvent: Pd nanoparticle stabilisation for sub-ppm Pd catalysis of Suzuki–Miyaura reactions of aryl bromides, *Chem. Commun.*, 2013, **49**, 8169-8171.

31 C. Ornelas, L. Salmon, J. R. Aranzaes and D. Astruc, Catalytically Efficient Palladium Nanoparticles Stabilised by Click" Ferrocenyl Dendrimers, *Chem. Commun.*, 2007, **46**, 4946-4948.

32 V. Polshettivar, R. Luque, A. Fihri, H. B. Zhu, M. Bouhrara and J. M. Basset, Magnetically Recoverable Nanocatalysts, *Chem. Rev.*, 2011, **111**, 3036-3075.

33 D. Astruc, Palladium catalysis using dendrimers: molecular catalysts versus nanoparticles, *Tetrahedron Asym.*, 2010, **21**, 1041-1054.

34 Q. Wang, F. Fu, S. Yang, M. Martinez, M. Ramirez, S. Moya, L. Salmon, J. Ruiz and D. Astruc, Dramatic Synergy in CoPt Nanocatalysts sed by "Click" Dendrimers for Evolution of Hydrogen from Hydrolysis of Ammonia Borane, *ACS Catal.*, 2019, **9**, 1110-1119.

35 K. C. Brown, J. E. Corbett and N. P. Loveless, Spectrophotometric studies on the protonation of hydroxy and aminophenazines in aqueous solution, *Spectrochim. Acta Part A Mol. Spectrosc.*, 1979, **35**, 421–423.

36 S. Fornera and P. Walde, Spectrophotometric quantification of horseradish peroxidase with o-phenylenediamine, *Anal. Biochem.*, 2010, **407**, 293–295.

37 J. Xie, H. Cao, H. Jiang, Y. Chen, W. Shi, H. Zheng and Y. Huang, Co_3O_4-reduced graphene oxide nanocomposite as an effective peroxidase mimetic and its application in visual biosensing of glucose, *Anal. Chim. Acta.*, 2013, **796**, 92–100.

38 F. Vetr Z. Moradi-Shoeili and S. Özkar, Oxidation of o-phenylenediamine to 2, 3-diaminophenazine in the presence of cubic ferrites MFe_2O_4 (M = Mn, Co, Ni, Zn) and the application in colorimetric detection of H_2O_2, *Appl. Organometal Chem.*, 2018, **32**, 4465-4475.

39 Z. Wang, M. Chen, J. Shu and Y. Li, One-step solvothermal synthesis of $Fe_3O_4@Cu@Cu_2O$ nanocomposite as magnetically recyclable mimetic peroxidase, *J. Alloys Compd.*, 2016, **682**, 432–440.

40 J. Guan, J. Peng and X. Jin, Synthesis of copper sulfide nanorods as peroxidase mimics for the colorimetric detection of hydrogen peroxide, *Anal. Methods.*, 2015, **7**, 5454–5461.

41 L. Lin, Y. Xiao, Y. Wang, Y. Zeng, Z. Lin and X. Chen, Hydrothermal synthesis of nitrogen and copper co-doped carbon dots with intrinsic peroxidase-like activity for colorimetric discrimination of phenylenediamine isomers, *Microchim. Acta.*, 2019, **186**, 288-296.

42 L. Chen, B. Sun, X. Wang, F. Qiao and S. Ai, 2D ultrathin nanosheets of Co-Al layered double hydroxides prepared in l-asparagine solution: enhanced peroxidase-like activity and colorimetric detection of glucose, *J. Mater. Chem. B*, 2013, **1**, 2268–2274.

43 Y. Tao, M. Li, B. Kim and D. Auguste, Incorporating gold nanoclusters and target directed liposomes as a synergistic amplified colorimetric sensor for HER2-positive breast cancer cell detection, *Theranostics*, 2017, **7**, 899-912.

44 L. Liang, S Ge, L. Li, F Liu and J. Yu. Microfluidic paper-based multiplex colorimetric immunodevice based on the catalytic effect of $Pd/Fe_3O_4@C$ peroxidase mimetics on multiple chromogenic reactions. *Anal. Chim Acta*, 2015, **3**, 70-76.

ARTICLE

Professor Didier Astruc
ISM, UMR CNRS N°5255, University of Bordeaux,
351 Cours de la Libération, 33405 Talence Cedex, France
Tel 00 33 6 08 09 23 97. E-mail : didier.astruc@u-bordeaux.fr

To

Prof. Song Gao
Editor-in-Chief, *Inorganic Chemistry Frontiers*

Bordeaux, March 31, 2021

Dear Prof. Song Gao

Title: "Click" dendrimer-Pd nanoparticle assemblies as enzyme mimics: Catalytic *o*-phenylenediamine oxidation and application to colorimetric H_2O_2 detection

Authors: Yue Liu, Renata Pereira Lopes, Tanya Luedtke, Desire Di Silvio, Sergio Moya, Jean-René Hamon, Didier Astruc

   Please find herewith the above manuscript that we are submitting as a full paper to *Inorganic Chemistry Frontiers*. This work has not been submitted anywhere, and there are no conflicts of interest. All the authors have approved the manuscript and agree with its submission to *Inorganic Chemistry Frontiers*.

   This manuscript reports the original work concerning the mimics of peroxidase enzyme by "click" dendrimer-palladium nanoparticle (PdNP) assemblies applied for the low-limit detection of hydrogen peroxide (H_2O_2) that is essential in biochemical analysis for application in biological and environmental processes. Therefore, advantage has been taken of the specific interaction between triazole tethers of the "click" dendrimers and the surface of intradendritically encapsulated PdNPs. This supramolecular nano-assembly selectively catalyses the oxidation of *o*-phenylenediamine using H_2O_2, allowing colorimetric H_2O_2 sensing at low concentration. Various parameters have been assessed to optimize this reaction, and comparison with literature reports indicate that this nanocatalyst is among the very best ones.

   We believe that these concepts and new finding should be of major interest to chemists and nano scientists in general, and in particular to the readers of *Inorganic Chemistry Frontiers*.

   Sincerely Yours,

   Didier Astruc
   Professor of Chemistry

"Click" dendrimer-Pd nanoparticle assemblies as enzyme mimics: Catalytic

o-phenylenediamine oxidation and application to colorimetric H$_2$O$_2$ detection

Yue Liu,[a] Renata Pereira Lopes,[a,b] Tanja Lüdtke,[c] Desire Di Silvio,[c] Sergio Moya,[c] Jean-René Hamon,[d] Didier Astruc[a]

[a]ISM, UMR CNRS N° 5255, Univ. Bordeaux, 33405 Talence Cedex, France.

---

[a].   ISM, UMR CNRS Nº 5255, Univ. Bordeaux, 33405 Talence Cedex, France. E-mail:
yue.liu@u-bordeaux.fr, didier.astruc@u-bordeaux.fr

[b].   Department of Chemistry, Universidade Federal de Viçosa, Viçosa/MG, Brazil, 36570-
900. E-mail: renataplmoreira@gmail.com

[c].   Soft Matter Nanotechnology Lab, CIC biomaGUNE, Paseo Miramón 182,
20014 Donostia-San Sebastián, Gipuzkoa, Spain

[d].   Institut des Sciences Chimiques, UMR CNRS 6226, Université de Rennes 1, 35042
Rennes Cedex, France

Electronic Supplementary Information (ESI)

1. Procedure for the preparations of the dendrimer-1 and dendrimer-2
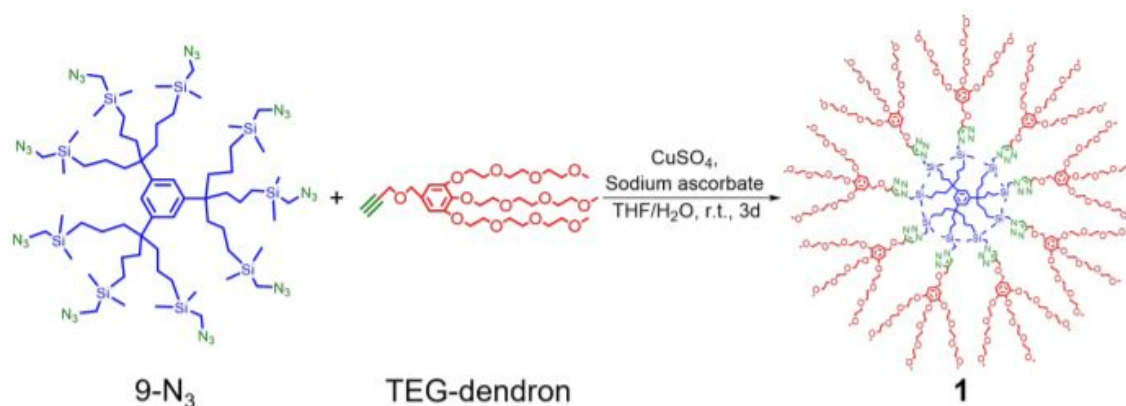
Scheme 1. Synthesis of dendrimer-**1**

Dendrimer **1** has been synthesized following previous reports. [S1, S2] 1,2 9-N$_3$ (see Scheme 1, 0.012 mmol,) and the TEG dendron (see Scheme 1, 0.13 mmol, 1.2 equiv. per branch) are dissolved in THF. CuSO$_4$.5H$_2$O is added (0.032 g, 0.13 mmol, 1.2 equiv. per branch, 1M in aqueous solution), followed by dropwise addition of a freshly prepared solution of sodium ascorbate (0.051 g, 0.26 mmol, 2.4 equiv. per branch, 1M in water solution) in order to set a 1:1 THF/water ratio. The reaction mixture is stirred for 3 days at 25 °C under N$_2$. After removing THF in vacuo, CH$_2$Cl$_2$ (100 mL) and an aqueous ammonia solution (2.0 M, 50 mL) are successively added. The mixture is allowed to stir for 10 minutes in order to remove all the Cu(II) trapped inside the dendrimer as [Cu(NH$_3$)$_2$(H$_2$O)$_2$][SO$_4$]. The organic phase is washed twice with water, and this operation is repeated three more times to ensure complete removal of copper ions. The organic phase is dried with sodium sulfate, and the solvent is removed *in vacuo*. The product is washed with 50 mL pentane several times in order to remove the excess of the dendron. Dendrimer **1** is obtained in 72.8 % yield. The procedure for the synthesis of dendrimer **2** is similar to that used for **1**, and use the procedure reported in reference S1, **2** is obtained in 70 % yield.
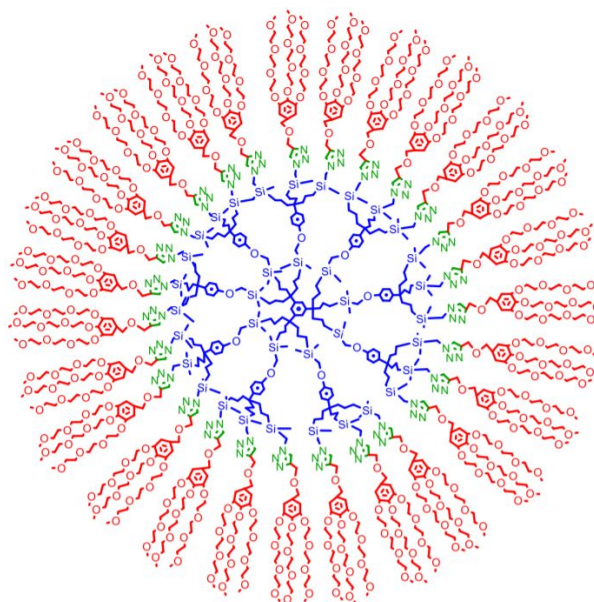
Dendrimer **2**

2. ^{1}H NMR of the dendrimer-1 and dendrimer-2

^{1}H NMR (CDCl$_3$, 300 MHz) d$_{ppm}$: 7.51 (CH-triazole), 6.99 (CH-arom. intern), 6.60 (CH-arom. extern), 4.63 (triazole-CH$_2$-O), 4.48 (O-CH$_2$-arom. extern), 3.85-4.15 (CH$_2$CH$_2$O-arom. extern), 3.80 (Si-CH$_2$-triazole), 3.53-3.77 (OCH$_2$CH$_2$O), 3.37-3.40 (CH$_3$O), 1.70 (CH$_2$CH$_2$CH$_2$Si), 1.13 (CH$_2$CH$_2$CH$_2$Si), 0.66 (CH$_2$CH$_2$CH$_2$Si), 0.07 (Si(CH$_3$)$_2$).
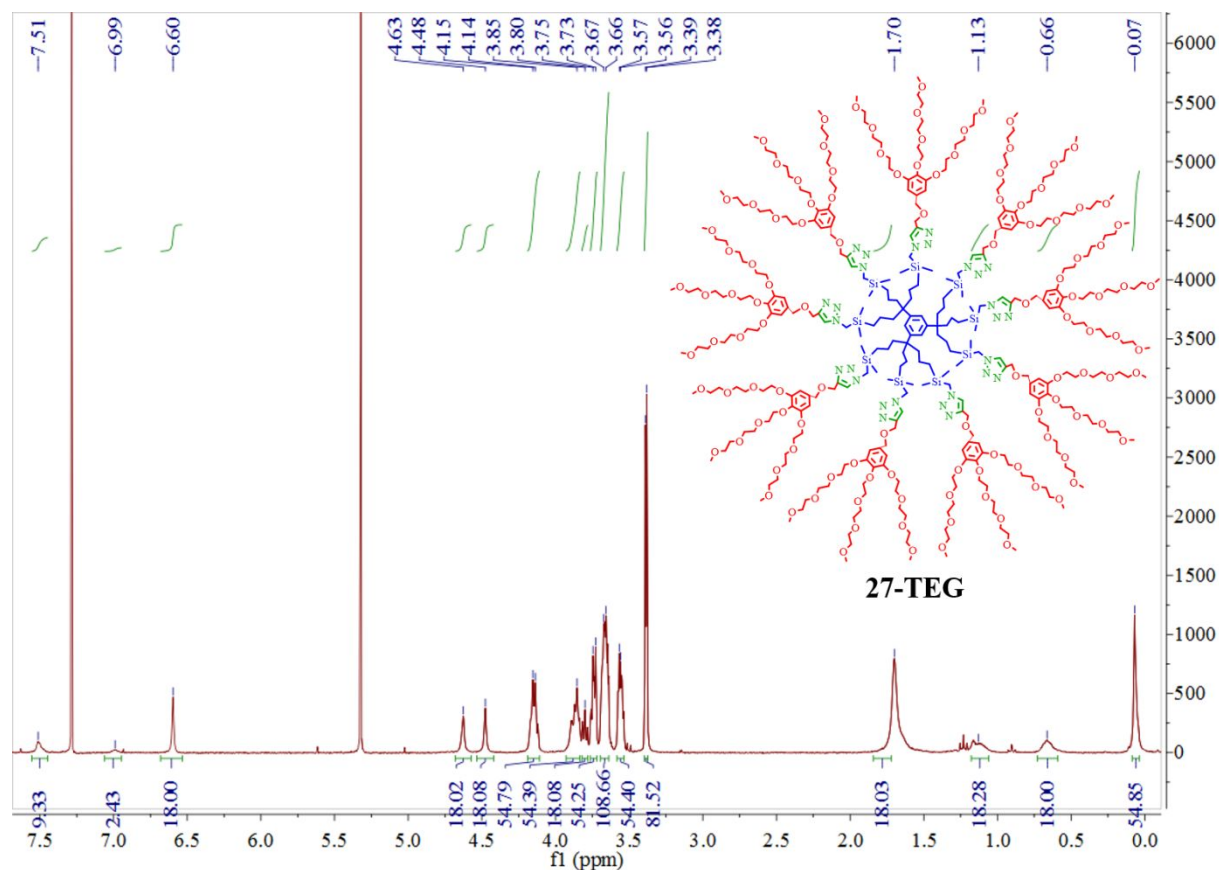
Figure S1. ^{1}H NMR spectrum of dendrimer-**1** in CDCl$_3$.

^{1}H NMR (CDCl$_3$, 300 MHz) d$_{ppm}$: 7.51 (CH-triazole), 6.89-7.15 (CH-arom. intern), 6.60 (CH-arom. extern), 4.64 (triazole-CH$_2$-O), 4.48 (O-CH$_2$-arom. extern), 3.85-4.15 (CH$_2$CH$_2$O-arom. extern), 3.80 (Si-CH$_2$-triazole), 3.56-3.74 (OCH$_2$CH$_2$O), 3.55 (CH$_2$O-arom. intern) 3.36-3.40 (CH$_3$O), 1.63 (CH$_2$CH$_2$CH$_2$Si), 1.12 (CH$_2$CH$_2$CH$_2$Si), 0.63 (CH$_2$CH$_2$CH$_2$Si), 0.06 (Si(CH$_3$)$_2$).
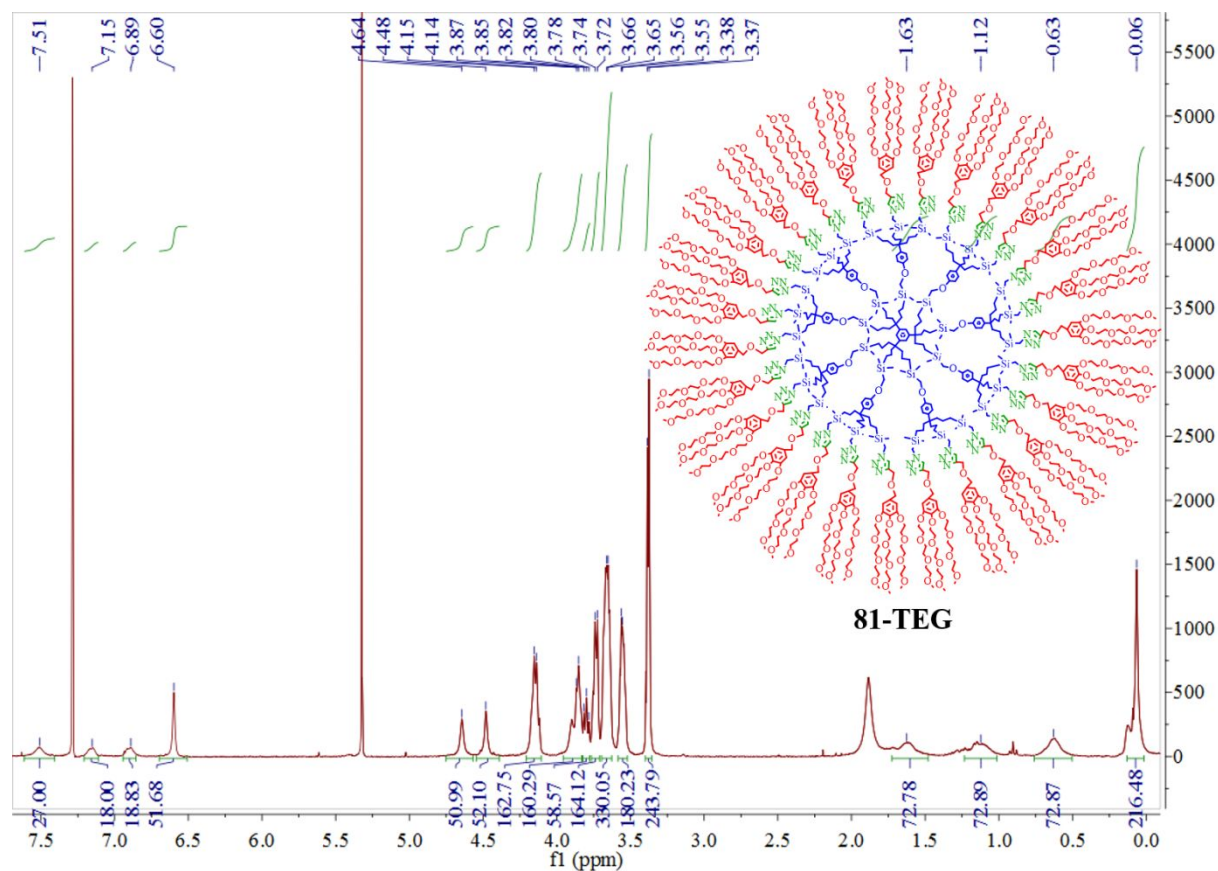

Figure S2. ^{1}H NMR spectrum of dendrimer-**2** in CDCl$_3$.

3. XPS experiments for the dendrimer-1-PdNPs and dendrimer-2-PdNPs.

XPS experiments were performed in a SPECS Sage HR 100 spectrometer with a non-monochromatic X-ray source (Magnesium Kα line of 1253.6 eV energy and 252 W), placed perpendicular to the analyzer axis and calibrated using the $3d_{5/2}$ line of Ag with a full width at half maximum (FWHM) of 1.1 eV.

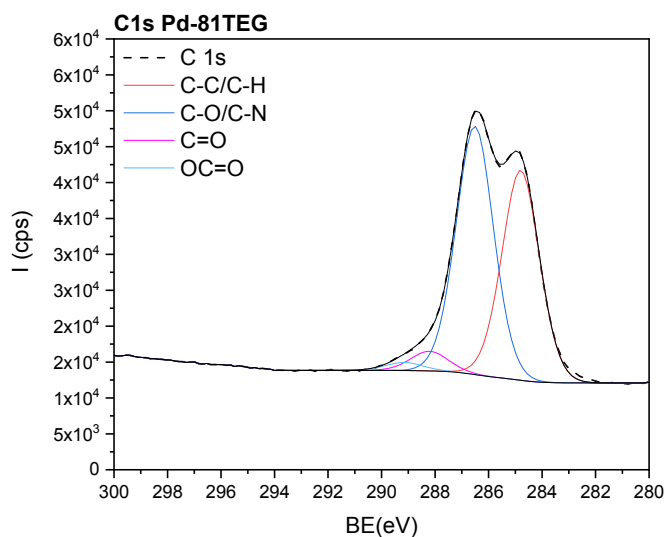**3.1 Carbon 1s region of the dendrimer-1-PdNPs and dendrimer-2-PdNPs.**

Figure S3. Carbon 1s region of dendrimer-**2**-PdNPs

Table S1 C 1s peak BE obtained by deconvolution and reported in Figure S3 and Figure S4.

	C-C/C-H (eV) [at%]	C-O/C-N (eV) [at%]	C=O (eV) [at%]	OC=O (eV) [at%]
Pd-27TEG	284.8 [61.2]	286.4 [32.3]	288.2 [4.2]	289.3 [2.3]
Pd-81TEG	284.8 [43.2]	286.5 [51.1]	288.2 [4.0]	289.2 [1.7]

3.2 Oxygen 1s region of the dendrimer-1-PdNPs and dendrimer-2-PdNPs.

The oxygen peak is generally wide and difficult to resolve discrimination of the different species. In the literature, the O-Metal bond is <530eV, C=O 530-531 eV, C-O and Si-O 531-533 eV, OC=O and C-OH and H_2O >534eV. Pd $3p_{3/2}$ BE can vary from 532 (Pd^0) eV up to 535 eV ($PdCl_2$).
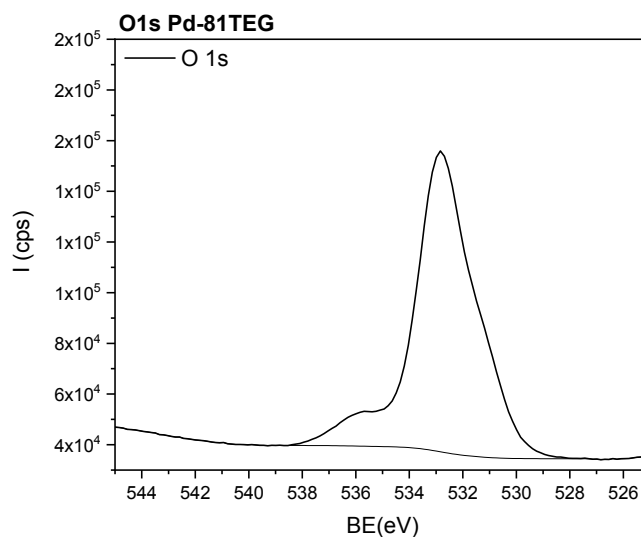
Figure S4. Oxygen 1s region of dendrimer-**2**-PdNPs

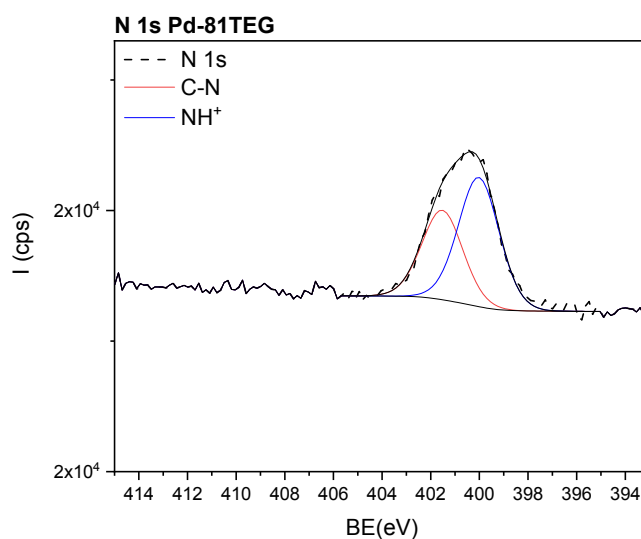### 3.3 Nitrogen 1s region of the dendrimer-1-PdNPs and dendrimer-2-PdNPs.

Figure S5. Nitrogen 1s region of dendrimer-**2**-PdNPs

Table S2 N 1s peak BE obtained by deconvolution and reported in Figure S7 and Figure S8.

	N-C (eV) [at%]	NH+ (eV) [at%]
Pd-27TEG	400.4 [100]	-
Pd-81TEG	400.0 [59]	401.5 [41]

3.4 Pd 3d region of the dendrimer-1-PdNPs and dendrimer-2-PdNPs.

Pd is readily reduced by X-ray and for this reason the acquisition time was reduced to minimum. The 3d region is represented by a doublet with average splitting of 5.3eV. Pd $3d_{5/2}$ is found below 335 eV in Pd^0 while Pd^{II} has higher BE. Several species, most likely made of Pd^{II}, were detected and indicated as (I) and (II).
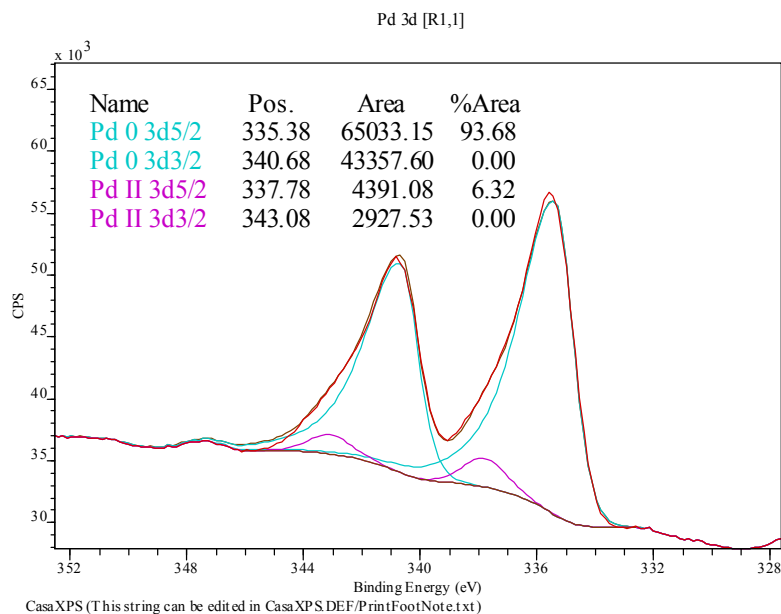

Pd 3d [R1,1]

Name	Pos.	Area	%Area
Pd 0 3d5/2	335.38	65033.15	93.68
Pd 0 3d3/2	340.68	43357.60	0.00
Pd II 3d5/2	337.78	4391.08	6.32
Pd II 3d3/2	343.08	2927.53	0.00

CasaXPS (This string can be edited in CasaXPS.DEF/PrintFootNote.txt)

Figure S6. Pd 3d region of dendrimer-**2**-PdNPs

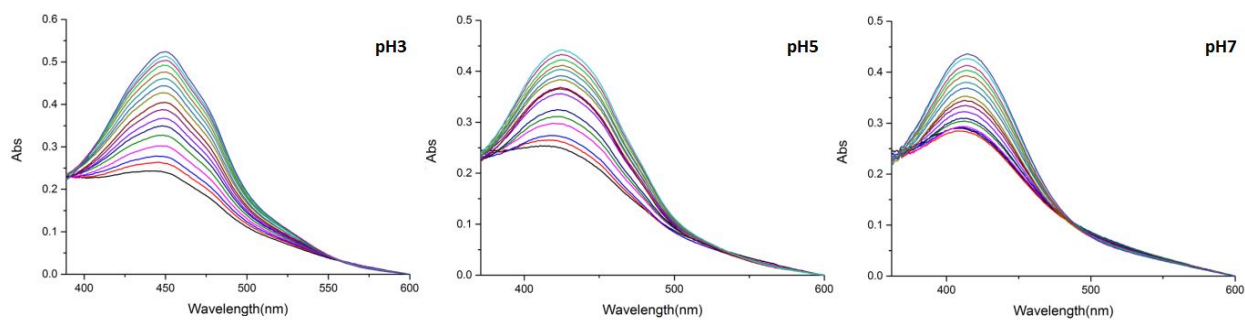## 4. *OPD oxidation catalyzed by dendrimer-1-PdNPs at various pH values.*

Fig. S7. OPD oxidation catalyzed by dendrimer-**1**-PdNPs at various pH.

General conditions: 0.1M OPD; 0.4 mL H_2O_2 30%; 2 mM dendrimer-**1**-PdNPs
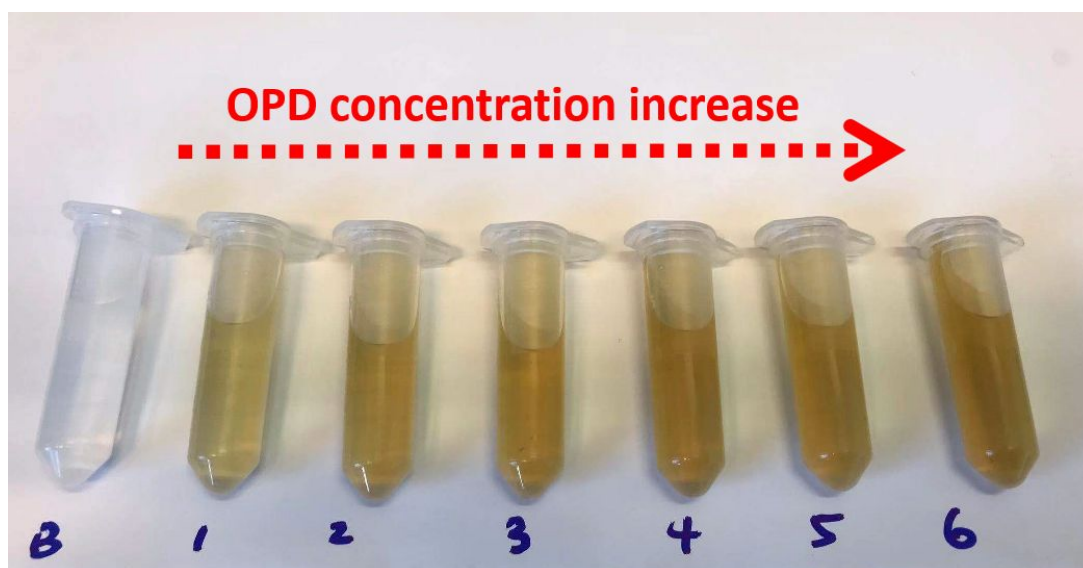
5. *Variation of OPD concentration*

Fig. S8. Color changes during oxidization of OPD catalyzed by dendrimer-**1**-PdNPs in the presence of OPD with increased concentrations.
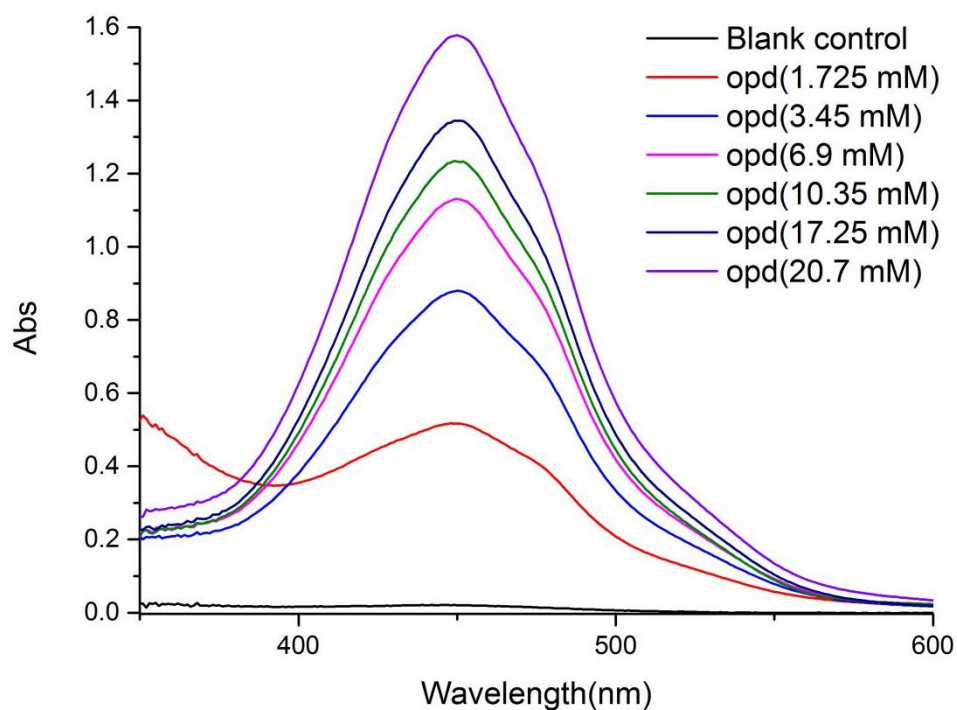

Fig. S9. Variation of OPD concentration during the catalytic oxidation by dendrimer-**1**-PdNPs.

General conditions: 0.4 mL H_2O_2 30%; 2 mM dendrimer-**1**-PdNPs

Table S3. Comparison of the apparent Michaelis–Menten constant (K_m)

and maximum reaction rate (V_m) for OPD as substrate

Material	C_{H2O2}	C_{cat}	$V_{max} \times 10^{-8}$ (M s^{-1})	K_m (mM)	Ref.
MnFe$_2$O$_4$	60 mM	0.06mg mL^{-1}	10.4	27.5	3
Cu-based carbon dots (Cu-CDs)	0.625 mM	0.05mg mL^{-1}	3.315	0.548	4
Co$_3$O$_4$	0.67 mM	0.05 nM	3.22	0.61	5
Fe$_3$O$_4$@Cu@Cu$_2$O	2.0 mM	0.05mg mL^{-1}	13.1	0.85	6
Horseradish peroxidase	0.625 mM	0.05mg mL^{-1}	0.12	1.8	4
dendrimer-1-PdNPs	0.4 mL	2 mM	0.151	3.06	This work

References

1 Q. Wang, F. Fu, A. Escobar, S. Moya, L. Salmon and D. Astruc, "Click" Dendrimer-Stabilized Nanocatalysts for Efficient Hydrogen Release upon Ammonia-Borane Hydrolysis. *ChemCatChem*, 2018, **10**, 2673-2680.

2 Q. Wang, F. Fu, S. Yang, M. Martinez, M. Ramirez, S. Moya, L. Salmon, J. Ruiz and D. Astruc, Dramatic Synergy in CoPt Nanocatalysts Stabilized by "click" Dendrimers for Evolution of Hydrogen from Hydrolysis of Ammonia Borane. *ACS Catal.,* 2019, **9**, 1110-1119.

3 F. Vetr, Z. Moradi-Shoeili and S. Özkar, Oxidation of *o*-phenylenediamine to 2, 3-diaminophenazine in the presence of cubic ferrites MFe_2O_4 (M= Mn, Co, Ni, Zn) and the application in colorimetric detection of H_2O_2, *Appl. Organometal. Chem*., 2018, **32**, 4465-4475.

4 D. Yang, Q. Li, S.K. Tammina, Z. Gao and Y. Yang, Cu-CDs/H_2O_2 system with peroxidase-like activities at neutral pH for the co-catalytic oxidation of *o* -phenylenediamine and inhibition of catalytic activity by Cr(III), *Sens. Actuators B. Chem.* 2020, **319**, 128273.

5 H. Jia, D. Yang, X. Han, J. Cai, H. Liu and W. He, Peroxidase-like activity of the Co_3O_4 nanoparticles used for biodetection and evaluation of antioxidant behavior, *Nanoscale*. 2016 , **8**, 5938–5945.

6 Z. Wang, M. Chen, J. Shu, Y. Li, One-step solvothermal synthesis of $Fe_3O_4@Cu@Cu_2O$ nanocomposite as magnetically recyclable mimetic peroxidase, *J. Alloys Compd*. 2016, 682, 432–440.